Evidence against reciprocal regulation of Ca^{2+} entry by vasopressin in A7r5 rat aortic smooth-muscle cells

Lioubov I. BRUEGGEMANN*, Daniel R. MARKUN*, John A. BARAKAT*, Haiyan CHEN† and Kenneth L. BYRON*[1]

*Department of Medicine, Cardiovascular Institute, Loyola University Chicago, Maywood, IL 60153, U.S.A., and †Department of Physiology, Cardiovascular Institute, Loyola University Chicago, Maywood, IL 60153, U.S.A.

Recent studies by Moneer and Taylor [(2002) Biochem. J. **362**, 13–21] have proposed a reciprocal regulation of two Ca^{2+}-entry pathways by AVP ([Arg^8]-vasopressin) in A7r5 vascular smooth-amuscle cells. Their model proposes that AVP inhibits CCE (capacitative Ca^{2+} entry) and predicts a rebound of CCE after the removal of AVP. In the present study, we used whole-cell perforated patch-clamp techniques to measure I_{SOC} (store-operated current) corresponding to CCE in A7r5 cells. When 100 nM AVP is present, it activates I_{SOC} with no apparent rebound on removal of AVP. I_{SOC} activated by thapsigargin or cyclopiazonic acid was not inhibited by 100 nM AVP. We also used fura 2 fluorescence techniques to re-examine the model of Moneer and Taylor, specifically focusing on the proposed inhibition of CCE by AVP. We find that 100 nM AVP activates capacitative Mn^{2+} entry and does not inhibit thapsigargin- or cyclopiazonic acid-activated Mn^{2+} entry. Moreover, Ca^{2+} entry after depletion of intracellular Ca^{2+} stores is enhanced by AVP and we detect no rebound of Ca^{2+} or Mn^{2+} entry after AVP removal. On the basis of these findings, we conclude that AVP does not inhibit CCE in A7r5 cells.

Key words: A7r5 cells, calcium entry, fura 2, store-operated current, vascular smooth muscle, vasopressin.

INTRODUCTION

Non-selective cation channels have been implicated in vasoconstrictor actions as a mechanism for regulating Ca^{2+} entry in vascular smooth-muscle cells. Ca^{2+} entering the cytosol through these channels may directly activate cell contraction, and the inward current carried by Ca^{2+} and Na^+ may contribute to membrane depolarization for the activation of Ca^{2+} entry through L-type voltage-sensitive Ca^{2+} channels. We have demonstrated previously that AVP ([Arg^8]-vasopressin) elicits distinct Ca^{2+} signalling patterns depending on its concentration [1,2]. Ca^{2+} spiking involving L-type voltage-sensitive Ca^{2+} channels predominates at the low concentrations of AVP found in the systemic circulation [2]. The roles of non-selective cation channels in these effects of AVP are yet to be examined. It will be important to elucidate the ionic mechanisms governing AVP-stimulated Ca^{2+}-entry pathways to understand further their physiological functions.

Ca^{2+} entry, presumably through non-selective cation channels, has been studied in A7r5 vascular smooth-muscle cells using Ca^{2+}-sensitive fluorescent indicators in cells treated with nimodipine or verapamil to exclude contributions of L-type Ca^{2+} channels [1,3–6]. Byron and Taylor [1] identified two distinct pathways for Ca^{2+} entry activated by AVP in A7r5 cells: a CCE (capacitative Ca^{2+}-entry) pathway activated by the depletion of intracellular Ca^{2+} stores and an NCCE (non-capacitative Ca^{2+}-entry) pathway activated specifically by AVP and with differing ionic permeabilities when compared with CCE. Recent studies by Moneer et al. [3,6] have suggested that AVP activates the NCCE pathway while simultaneously inhibiting the CCE pathway.

In the present study, we have examined the electrophysiological correlation of CCE by studying the store-operated current I_{SOC} and its regulation by AVP. We find that I_{SOC} is activated by AVP in a manner that is not consistent with the reciprocal regulation proposed by Moneer and Taylor [3]. It should be noted that several results of Moneer et al. [3,6] differ from or directly contradict earlier results from the same laboratory. For example: (i) Byron and Taylor [1] demonstrated that AVP had no effect on capacitative Mn^{2+} entry, but Moneer and Taylor [3] reported that AVP inhibits capacitative Mn^{2+} entry by as much as 90 %; (ii) Broad et al. [4] reported that arachidonic acid had no effect on capacitative Mn^{2+} entry, whereas Moneer and Taylor [3] found that arachidonic acid inhibits CCE; (iii) Byron and Taylor [1] demonstrated that $[Ca^{2+}]_i$ responses to [AVP] $\geqslant$ 50 nM exhibited little plateau phase, whereas a pronounced and sustained increase of $[Ca^{2+}]_i$ ($\sim$300 nM above resting levels) is apparent in the results of Moneer and Taylor [3]; (iv) Byron and Taylor [1] found, using both cell populations and single cells, that AVP enhances Ba^{2+} entry beyond that stimulated by maximal store depletion, but Moneer and Taylor [3] reported that capacitative Ba^{2+} entry was decreased by AVP.

Because of the above-noted contradictions in the previous studies and because our electrophysiological results did not fit the reciprocal regulation model, we used fura 2 fluorescence methods to re-examine the CCE pathway and its regulation in A7r5 cells. Our present findings are consistent with the original findings of Byron and Taylor [1] and also support their conclusions that AVP directly activates an NCCE pathway that is relatively impermeable to Mn^{2+} and that AVP does not inhibit CCE [1]. The differences between the results of Moneer et al. [3,6] and our present and previous findings are discussed.

EXPERIMENTAL

A7r5 cell culture

A7r5 cells were propagated from low-passage stocks used in the studies of Byron and Taylor [1,7] and cultured as described

Abbreviations used: $[Ca^{2+}]_i$, cytosolic free Ca^{2+} concentration; AVP, [Arg^8]-vasopressin; BAPTA, bis(2-amino-5-bromophenoxy)ethane-*N*,*N*,*N*′,*N*′-tetra-acetic acid; CCE, capacitative Ca^{2+} entry; CPA, cyclopiazonic acid; NCCE, non-capacitative Ca^{2+} entry; fura 2/AM, fura 2 acetoxymethyl ester; NMDG, *N*-methyl-D-glucamine.

[1] To whom correspondence should be addressed (email kbyron@lumc.edu).

previously [8]. Cells were subcultured on to rectangular (9 mm × 22 mm, no. 1½) glass coverslips or plastic tissue culture flasks (Corning, Acton, MA, U.S.A.). For fura 2 fluorescence measurements, confluent cell monolayers grown on glass coverslips were used 2–5 days after plating. For electrophysiological recordings, cells grown on plastic were trypsinized (0.25 % trypsin and 1 % EDTA) and replated on 12 mm round glass coverslips. Cells were allowed to adhere for approx. 15 min and then transferred on to external solution for 30 min to 2 h before recording.

Patch-clamp

Whole-cell perforated- or ruptured-patch configurations were used to measure membrane currents under voltage-clamp conditions in single A7r5 cells. All experiments were performed at room temperature (23–25 °C) with continuous perfusion of external solution (perfusion rates of 1 ml/min; ~0.7 ml chamber volume).

The external solution for recording I_{SOC} contained (in mM): 100 NMDG (*N*-methyl-D-glucamine) aspartate, 20 calcium aspartate, 1 $MgCl_2$ and 10 Hepes (pH 7.3). Internal (pipette) solution contained (in mM): 90 caesium aspartate, 20 CsCl, 4.6 $MgCl_2$, 5 Hepes, 10 BAPTA-Cs_4 [where BAPTA stands for bis(2-amino-5-bromophenoxy)ethane-*N*,*N*,*N*′,*N*′-tetra-acetic acid; pH 7.2]. With no Ca^{2+} added, but assuming possible contamination from impure chemicals resulting in up to 10 μM total Ca^{2+}, we estimate the concentration of free Ca^{2+} in the internal solution to be less than 0.4 nM (calculated with WINMAXC software).

The conditions used were intended for maximal isolation of I_{SOC} from other currents, including another vasopressin-activated non-selective cation current, which was undetectably small in this external solution (results not shown). Cl^- currents were minimized by the use of an impermeant anion, aspartate (Asp^-). In addition, we conducted preliminary experiments (results not shown) to ensure that the inward current we measured was not carried by Cl^-: first, replacing 40 mM external Asp^- with 40 mM Cl^- did not affect the current–voltage relationship (it had the same inward rectification, current density and reversal potential as I_{SOC} that developed when Asp^- was the only anion in the external solution); secondly, replacement of all external Asp^- with Cl^- after I_{SOC} activation did not affect current densities or the reversal potential.

A well-accepted characteristic of I_{SOC} is that it is inhibited by lanthanides such as Gd^{3+}. CCE in A7r5 cells is also reportedly inhibited by low concentrations of Gd^{3+} (< 5 μM [3,4,6]). To demonstrate the Gd^{3+} sensitivity of I_{SOC} in A7r5 cells, we added 100 μM $GdCl_3$ to the external solution at the end of the experiment (e.g. Figures 1G, 2A and 2B). We estimate that the final concentration of free Gd^{3+} is in the 1–5 μM range (calculated with WINMAXC software using Gd-aspartate binding constants kindly provided by C. Patton, Stanford University). Inhibition of the inward current by micromolar free Gd^{3+} is consistent with its identification as I_{SOC} and also additionally distinguishes it from Cl^- currents, which are generally lanthanide-insensitive [9,10].

Nimodipine (0.5 μM) was present in all external solutions to inhibit L-type Ca^{2+} channels. Spermine chloride (100 μM) was also included to block the Mg^{2+}-inhibitable current I_{MIC} [11]. Osmolality of all solutions was adjusted to 270 mosmol/l with D-glucose. For membrane patch perforation, 200 μg/ml amphotericin B in the internal solution was used.

Experiments in whole-cell perforated patch configuration were started with series resistance $R_s < 30$ MΩ; cells with an abrupt decrease in R_s were discarded. Recording of I_{SOC} in ruptured patch configuration was started 30 s after break-in. Voltage-clamp command potentials were generated using an Axopatch 200B amplifier under the control of PCLAMP8 software. Time courses of I_{SOC} development during exposure to 1 and 100 nM AVP, 10 μM CPA (cyclopiazonic acid), 1 μM thapsigargin or cell dialysis with 10 mM internal BAPTA were recorded every 10 s by a ramp voltage protocol (from + 85 to − 115 mV starting from a − 15 mV holding potential). Whole-cell currents were digitized at 10 kHz, filtered at 5 kHz and analysed off-line. Currents were normalized to membrane capacitance. Whole-cell capacitance was compensated. Liquid junction potentials were calculated using junction potential calculator provided by PCLAMP8 software and subtracted off-line. Results are presented as means ± S.E.M.

$[Ca^{2+}]_i$ measurements

A7r5 cells were grown to confluence on glass coverslips. Coverslips were washed twice with control medium (135 mM NaCl, 5.9 mM KCl, 1.5 mM $CaCl_2$, 1.2 mM $MgCl_2$, 11.5 mM glucose and 11.6 mM Hepes, pH 7.3) and then incubated in the same medium with 4 μM fura 2/AM (fura 2 acetoxymethyl ester), 0.1 % BSA and 0.02 % Pluronic F127 detergent for 90–120 min at 25–30 °C in the dark. The cells were then washed twice and incubated in the dark in control medium (or pretreated with drugs) for 0.5–5 h before the start of the experiment. Fura 2 fluorescence (at 510 nm) was measured in cell populations with a PerkinElmer LS50B fluorescence spectrophotometer. Background fluorescence was determined at the end of the experiment by quenching the fura 2 fluorescence for 10–15 min in the presence of 1 μM ionomycin and 6 mM $MnCl_2$ in Ca^{2+}-free medium. After background fluorescence was subtracted, the ratio of fluorescence at 340 nm excitation to that at 380 nm was calculated and calibrated in terms of $[Ca^{2+}]_i$ as described previously [8].

Mn^{2+}-entry measurements

The rates at which Mn^{2+} enters the cells to quench fura 2 fluorescence were measured in cell populations after excitation at 358 nm, the wavelength that was empirically determined to be minimally sensitive to changes in $[Ca^{2+}]$. Changes in fluorescence intensity were measured while 150 μM $MnCl_2$ was present in Ca^{2+}-free control medium ($CaCl_2$ was omitted). Rates of fluorescence quench were determined using least-squares linear regression analysis (SigmaPlot 2000 software; SPSS, Chicago, IL, U.S.A.) of the change in emitted fluorescence in 1 min time periods (120 data points). Mn^{2+} entry was also measured in individual cells using a microscope-based digital image analysis system (Compix, Cranberry Township, PA, U.S.A.) that allowed for recording from approx. 10–15 cells within the microscope field. Sequential excitation at 340, 359 and 380 nm allowed simultaneous recording of Mn^{2+} entry (at 359 nm) and $[Ca^{2+}]_i$ (as indicated by changes in the 340:380 fluorescence ratio). All three wavelengths were recorded at acquisition rates of approx. 1 s^{-1}. Fluorescence intensity in single cells was measured using Compix SimplePCI software. For the analysis of Mn^{2+}-entry rates, fluorescence intensity after excitation at 359 nm (F) was normalized to the mean fluorescence recorded for 60 s, just before the addition of $MnCl_2$ (F_0); regression analysis from 2 min periods of normalized fluorescence (F/F_0) was used to estimate quench rates.

Materials

Amphotericin B was obtained from Calbiochem (La Jolla, CA, U.S.A.); AVP, [β-mercapto-β,β-cyclopentamethylenepropionyl^1, O-Et-Tyr^2, Val^4, Arg^8]-vasopressin, CPA, ionomycin, nimodipine, spermine chloride and thapsigargin were obtained from Sigma-Aldrich (St. Louis, MO, U.S.A.); fura 2/AM and Pluronic F127 were from Molecular Probes (Eugene, OR, U.S.A.).

LOE 908 was generously provided by Boehringer Ingelheim Pharmaceuticals (Ridgefield, CT, U.S.A.). Solubilization of LOE 908 was accomplished by preparing a 10 mM stock solution in

deionized water and then adding the appropriate volume of this stock to a volume of control medium before adjusting the pH to its final value.

RESULTS

We used electrophysiological techniques to measure I_{SOC} activated by depletion of Ca^{2+} stores. As shown in Figure 1(A), I_{SOC} is activated incrementally by the addition of 1 and 100 nM AVP and it stabilizes after the addition of 10 μM CPA, a reversible inhibitor of the sarco/endoplasmic reticulum Ca^{2+}-ATPase. I_{SOC} activity reverses rapidly on washout of CPA (Figure 1A). The same inwardly rectifying current developed as a result of passive emptying of Ca^{2+} stores with 1 μM thapsigargin (irreversible inhibitor of sarcoplasmic reticulum Ca^{2+}-ATPase; Figures 1C and 1D) or by cell dialysis with 10 mM BAPTA (< 1 nM free Ca^{2+} in the pipette) in the ruptured patch configuration (Figures 1E and 1F).

I_{SOC} activated by emptying of Ca^{2+} stores with AVP, CPA, thapsigargin or BAPTA have similar current densities measured at -115 mV (-0.60 ± 0.10 pA/pF AVP-activated I_{SOC}, $n = 6$; -0.49 ± 0.10 pA/pF thapsigargin-activated I_{SOC}, $n = 8$; -0.55 ± 0.03 pA/pF BAPTA-activated I_{SOC}, $n = 26$; -0.39 ± 0.05 pA/pF CPA-activated I_{SOC}, $n = 5$), have the same-shaped I–V curves, reversed at the same voltage and were each blocked by Gd^{3+}.

Replacement of 100 mM $NMDG^+$ in the external solution with 100 mM Na^+ did not alter the reverse potential or current density (Figure 1G), suggesting that I_{SOC} is relatively selective for Ca^{2+} compared with Na^+. In agreement with fura 2 fluorescence measurements of CCE, I_{SOC} is insensitive to 30 μM LOE 908 (Figure 1H), a channel-blocking drug that was reported to inhibit NCCE without affecting CCE [3]. On the basis of its activation by treatments that actively or passively deplete intracellular Ca^{2+} stores, its ability to conduct Ca^{2+}, its sensitivity to μM Gd^{3+} and insensitivity to LOE 908, we hypothesize that I_{SOC} corresponds to the CCE pathway identified by fura 2 fluorescence studies.

On the basis of this hypothesis, the reciprocal regulation model of Moneer et al. [3,6] would predict that I_{SOC} would be active only after AVP removal and that AVP would inhibit thapsigargin-activated I_{SOC}. Using perforated patch whole-cell voltage clamp, we find that I_{SOC} is active in the presence of 100 nM AVP, with no apparent rebound on the removal of AVP (Figure 2A). We also found that thapsigargin-activated I_{SOC} is not inhibited by 100 nM AVP (Figure 2B).

To examine the apparent disagreement between the electrophysiology results and the reciprocal regulation model proposed by Moneer and Taylor [3], we used fura 2 fluorescence techniques, specifically focusing on the proposed inhibition of CCE by AVP. Previous studies [1] suggested that the CCE pathway is permeable to Mn^{2+}, whereas the NCCE pathway does not conduct Mn^{2+}. The reciprocal regulation theory [3] would predict that, during AVP exposure, there would be little enhancement of Mn^{2+} entry, but a robust increase in Mn^{2+} entry after the removal of AVP. We found that Mn^{2+} entry was significantly increased in the presence of 100 nM AVP (by 4.5 ± 1.2-fold, $n = 4$, $P < 0.01$, paired t test) and there was no rebound of Mn^{2+} entry after AVP removal (Figure 3). The AVP-stimulated Mn^{2+} entry may be attributed to CCE since (i) it did not require continued receptor activation (the stimulated rate was maintained after the removal of AVP in the Ca^{2+}-free medium) and (ii) brief exposure to extracellular Ca^{2+} (to refill partially the Ca^{2+} stores) significantly decreased the rate of Mn^{2+} entry (by 58 ± 4 %, $n = 3$, $P < 0.05$; Figures 3B and 3C).

The question of whether AVP inhibits Mn^{2+} entry after store depletion was also re-examined. Mn^{2+} entry was measured before

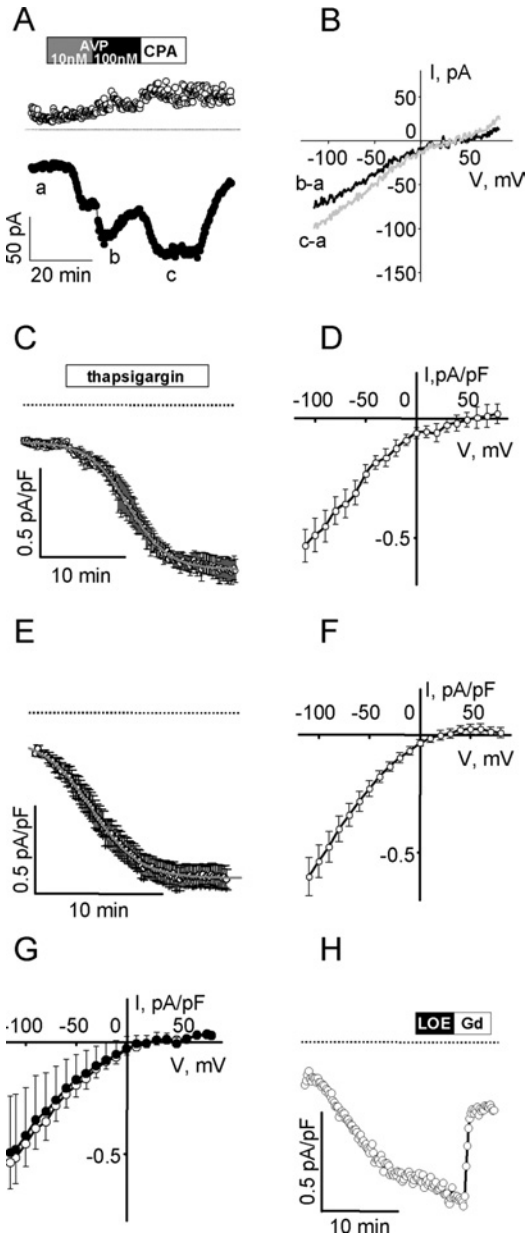

Figure 1 I_{SOC} in A7r5 vascular smooth-muscle cells

(**A**) Representative measurements of I_{SOC} development in an A7r5 cell with 171.5 pF capacitance (C) during sequential application of 1 nM AVP (15 min, grey box), 100 nM AVP (15 min, black box) and 10 μM CPA (15 min, white box) followed by washout of CPA. Drugs were applied after stable recording of the resting current for 5 min. Current was recorded with a ramp voltage protocol (from +85 mV to −115 mV) from −15 mV holding potential every 10 s. Inward currents measured at −115 mV (●) and outward current measured at +85 mV (○) are presented. The dotted line indicates 0 current level. (**B**) Current–voltage relationships of AVP-activated (black line) and CPA-activated (grey line) I_{SOC} recorded with the ramp voltage protocol at the time points indicated on (**A**) after subtraction of the resting current. Results are representative of at least three similar experiments. (**C**, **D**) Mean of perforated patch recordings ($n = 3$) of inwardly rectifying current activated as a result of passive emptying of Ca^{2+} stores with 1 μM thapsigargin (irreversible inhibitor of sarcoplasmic reticulum Ca^{2+}-ATPase) and the corresponding I–V curve of Gd^{3+}-sensitive portion of current respectively. Time to half-maximal activation was 12.39 ± 0.04 min. (**E**, **F**) The mean inwardly rectifying current that developed during dialysis of cells with 10 mM BAPTA (ruptured patch recordings, $n = 12$) and the corresponding I–V curve. Time to half-maximal activation was 4.92 ± 0.05 min. (**G**) Switching external monovalent cations do not affect maximal I_{SOC} (activated by dialysis with 10 mM BAPTA). Mean I–V curves recorded in 20 mM Ca^{2+} + 100 mM $NMDG^+$ (○, $n = 4$) and 20 mM Ca^{2+} + 100 mM Na^+ external solution (●, $n = 4$). (**H**) I_{SOC} activated by BAPTA dialysis was insensitive to 30 μM LOE 908, but was inhibited by the addition of 100 μM $GdCl_3$ ($C = 174.5$ pF, representative of four experiments).

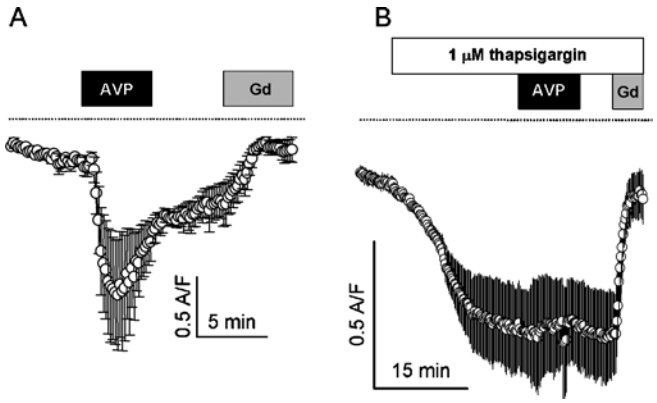

Figure 2 Effects of AVP on I_{SOC} in A7r5 vascular smooth-muscle cells

(**A**) Time course of I_{SOC} development was measured as described above; inward currents at −115 mV are presented as means ± S.E.M. ($n = 5$; capacitances in the range 45.5–159 pF). Boxes indicate application of 100 nM AVP and 100 μM $GdCl_3$. Dotted lines indicate 0 current level. (**B**) AVP (100 nM) did not inhibit I_{SOC} induced by passive depletion of Ca^{2+} store with 1 μM thapsigargin. Inward currents measured at −115 mV are presented as means ± S.E.M. ($n = 4$; capacitances in the range 219–432 pF). Boxes indicate application of 1 μM thapsigargin, 100 nM AVP and 100 μM $GdCl_3$.

or during exposure to CPA; CPA stimulated Mn^{2+} entry by 7.4 ± 0.8-fold ($n = 3$). No change in Mn^{2+} entry was observed when AVP (100 nM) was added after the stabilization of CPA-activated Mn^{2+} entry (8.0 ± 0.8-fold increase over basal, $n = 3$, $P > 0.5$ compared with CPA alone; Figure 4). These results are consistent with the conclusion of Byron and Taylor [1] that AVP does not inhibit capacitative Mn^{2+} entry, but cannot be readily reconciled with the results of Moneer and Taylor [3].

A7r5 cells were not derived by cloning [12] and therefore might be expected to display heterogeneity among cells in a population. We used single-cell imaging techniques to examine the heterogeneity of single-cell responses using a pretreatment method established by Byron and Taylor [1] and also used by Broad et al. [4] and Moneer and Taylor [3]. A7r5 cells are pretreated with a combination of ionomycin (1 μM) and thapsigargin (500 nM) to deplete fully the intracellular Ca^{2+} stores. The effectiveness of this treatment is demonstrated in Figure 7(A) where a robust Ca^{2+} release response to 100 nM AVP in untreated cells is compared with an undetectable Ca^{2+} release in the ionomycin/thapsigargin-pretreated cells. Figure 5(A) shows representative recordings of Mn^{2+} entry in individual A7r5 cells in the absence (upper left panels) or presence of 100 nM AVP (upper right panels). Capacitative Mn^{2+} entry produced a steady decrease in fura 2 fluorescence measured at the Ca^{2+}-insensitive wavelength (359 nm; Figure 5A, upper panels), which was not altered by the presence of 100 nM AVP. The Ca^{2+}-sensitive fluorescence ratio measured in the same cells (340:380; Figure 5A, lower panels) confirms that AVP did not detectably release additional Ca^{2+} from intracellular stores. Analysis of 102 cells from four independent experiments indicates that there was no effect of AVP on mean Mn^{2+}-entry rates (Figure 5B). We also examined the distribution of rates among individual cells comparing untreated and AVP-treated groups (Figure 5C). There was no significant difference in the distribution of rates, although there was a tendency towards a time-dependent decrease in quench rates in the controls, which was decreased by AVP, contrary to the predictions of the reciprocal regulation model.

Results of Broad et al. [4] and Moneer and Taylor [3] indicate that 1 μM Gd^{3+} selectively blocks CCE and 30 μM LOE 908 selectively blocks NCCE. Moneer and Taylor [3] report a robust

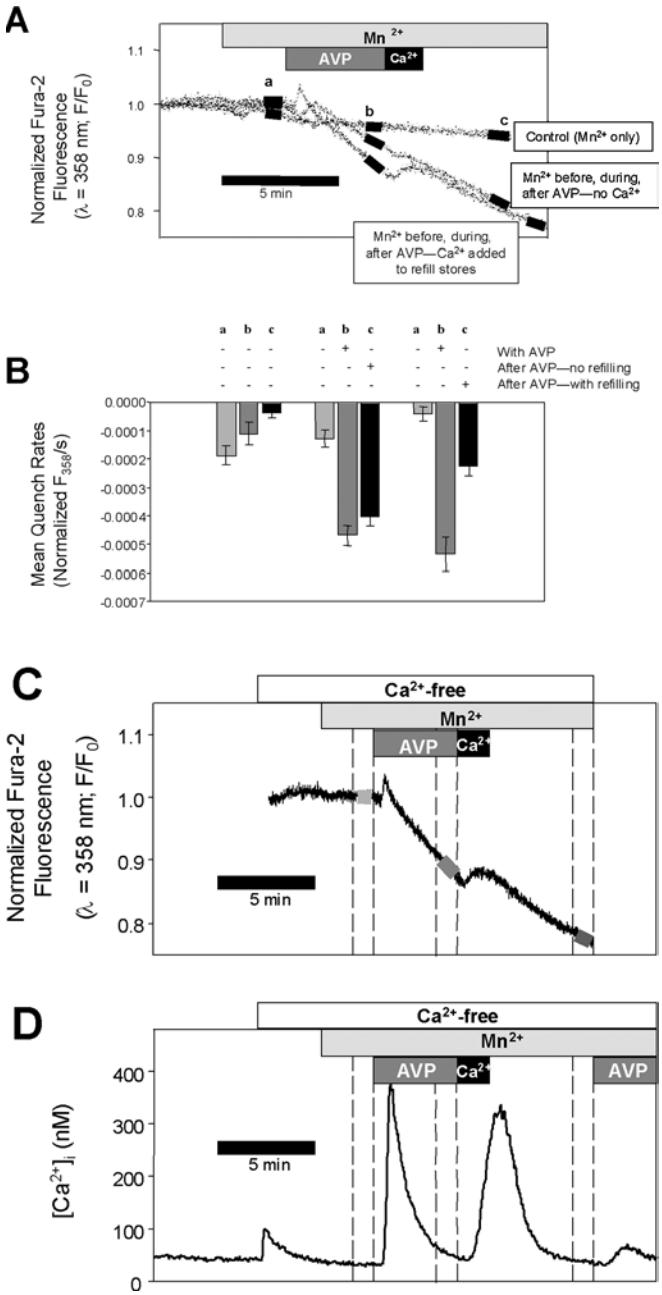

Figure 3 AVP stimulates Mn^{2+} entry: no rebound after AVP removal

(**A**) Unidirectional Mn^{2+} entry was measured at three time points (labelled a, b and c) in fura 2-loaded A7r5 cell monolayers based on the rate of quench of fura 2 fluorescence ($\lambda_{ex} = 358$ nm). Three sets of experiments were performed, represented by the three labelled traces in the top panel: the time course of Mn^{2+} entry in Ca^{2+}-free medium without any treatment (Control); the time course of Mn^{2+} entry before, during and after treatment with 100 nM AVP; the time course of Mn^{2+} entry before and during 100 nM AVP and after a brief introduction of 10 mM $CaCl_2$ to allow partial refilling of the intracellular Ca^{2+} stores. (**B**) The rates of fluorescence quench were measured (linear regression) at each of the three time points (black bars superimposed on traces on **A**) for each set of experiments ($n = 3$–4) and are summarized in the bar graph. The results indicate that capacitative Mn^{2+} entry is enhanced while AVP is present and is not further increased after AVP removal. (**D**) Changes in $[Ca^{2+}]_i$ that occur during the treatments for the third set of Mn^{2+} quench experiments (AVP followed by Ca^{2+}). $[Ca^{2+}]_i$ was estimated from the 340:380 fura 2 fluorescence ratios recorded from a different coverslip treated with the same solutions. In this case, the cells were exposed a second time to AVP to demonstrate that transient exposure to extracellular Ca^{2+} enabled the subsequent additional release of intracellular Ca^{2+}. The representative Mn^{2+}-entry recording is aligned temporally on (**C**) above the $[Ca^{2+}]_i$ recording, demonstrating that the rates of quench were determined at those time points when cytosolic $[Ca^{2+}]$ was low and would not interfere with the Mn^{2+}-entry measurements.

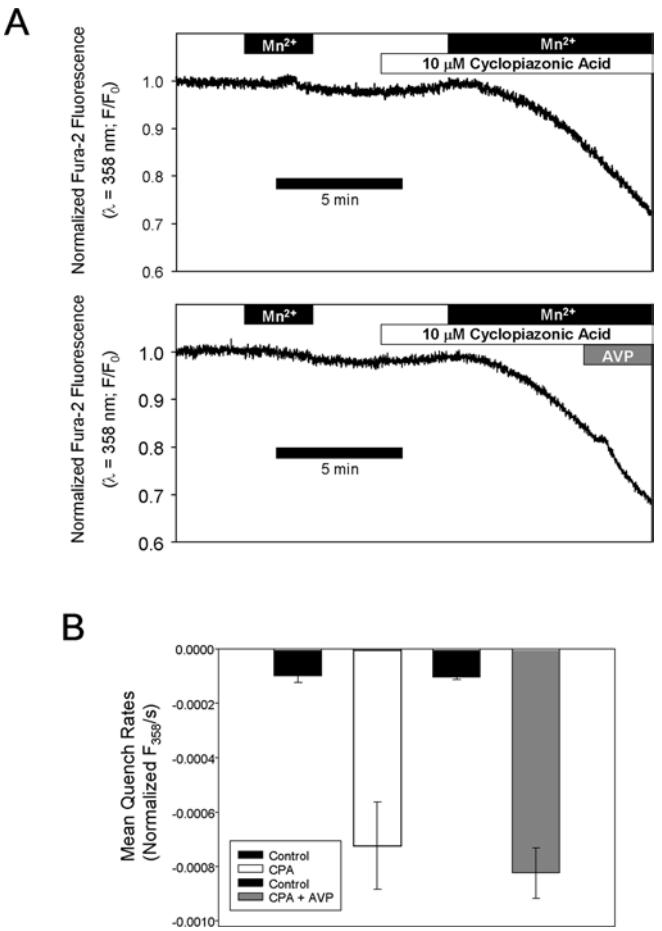

Figure 4 AVP does not inhibit CPA-activated Mn^{2+} entry

(**A**) Quench of fura 2 fluorescence due to unidirectional Mn^{2+} entry was measured in A7r5 cell populations before or during exposure to 10 μM CPA. CPA robustly increases Mn^{2+} entry and the rates of entry were not different when 100 nM AVP was added after maximal activation of Mn^{2+} entry by CPA. (**B**) Quench rates were estimated by least-squares regression analysis of the fluorescence recording during the final 60 s of each Mn^{2+} exposure; results represent the means for three independent experiments (error bars indicate S.E.M.).

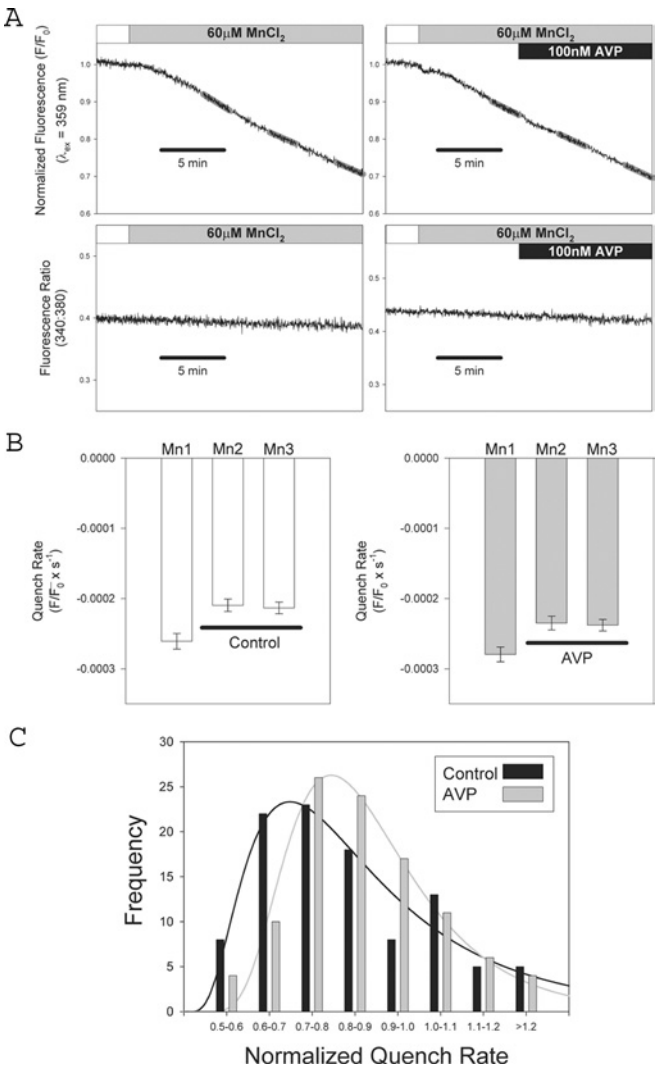

Figure 5 Analysis of store-operated Mn^{2+} entry in single cells: no effect of AVP

(**A**) Representative recordings of fura 2 fluorescence from single A7r5 cells pretreated with 500 nM thapsigargin + 1 μM ionomycin; upper panels show the quench of fura 2 fluorescence due to unidirectional Mn^{2+} entry at 359 nm excitation; lower panels show 340:380 ratios recorded simultaneously from the same cells. Right panels show responses recorded from a cell treated with 100 nM AVP (black bar). Linear regression analysis was used to measure fluorescence quench rates at three time points (indicated by grey regression lines labelled Mn1, Mn2 and Mn3 superimposed on traces). (**B**) Summarized data from 102 cells (51 untreated controls and 51 treated with 100 nM AVP); quench rates measured at each of the three time points indicated above (mean $\pm$ S.E.M.; no significant difference between control and AVP-treated). (**C**) Histogram analysis of the distribution of rates comparing control and AVP-treated cells. For each cell, the quench rates measured at time points Mn2 and Mn3 were normalized by dividing by the rates measured at Mn1. There was no significant difference in normalized quench rates between control and AVP-treated (Mann–Whitney Rank Sum Test, $P > 0.05$).

rebound of $[Ca^{2+}]_i$ after the removal of 200 nM AVP in the presence of 30 μM LOE 908, which they attribute to CCE. Using the same treatment method [same durations of treatment and concentrations of drugs and AVP, same perfusion rate (17 ml/min), addition of 100 nM [β-mercapto-β,β-cyclopentamethylenepropionyl^1, O-Et-Tyr^2, Val^4, Arg^8]-vasopressin, a V_{1a} vasopressin receptor antagonist, at the time of AVP washout [3], we found no rebound of $[Ca^{2+}]_i$ after the removal of AVP (200 nM; Figure 6). Gd^{3+} (1 μM) had little effect on AVP-induced $[Ca^{2+}]_i$ responses (Figure 6B). LOE 908 (30 μM) inhibited the $[Ca^{2+}]_i$ response to AVP, but no rebound Ca^{2+} transient was observed at the time of AVP removal (Figure 6C).

Moneer et al. [6] reported that AVP treatment nearly abolishes the Ca^{2+} transient that results when extracellular Ca^{2+} is reintroduced after the depletion of intracellular Ca^{2+} stores. We performed a set of experiments in which intracellular Ca^{2+} stores were first depleted with 500 nM thapsigargin and 1 μM ionomycin in Ca^{2+}-free medium (a similar method was used by Moneer et al. [6]). Fura 2 fluorescence ratios were then recorded during the reintroduction of extracellular Ca^{2+} (1.5 mM) without or at various times after the addition of 100 nM AVP (Figure 7). In three sets of experiments, the mean peak $[Ca^{2+}]_i$ response was at least 30 % larger, at all time points after AVP addition, compared with the control response measured in the absence of AVP. The enhanced peak is consistent with the activation of an additional Ca^{2+}-entry pathway (NCCE) by AVP, but inconsistent with the reciprocal regulation model of Moneer et al. [3,6].

DISCUSSION

Our present findings confirm earlier results from Byron and Taylor [1] demonstrating that AVP activates capacitative Ca^{2+} or Mn^{2+}

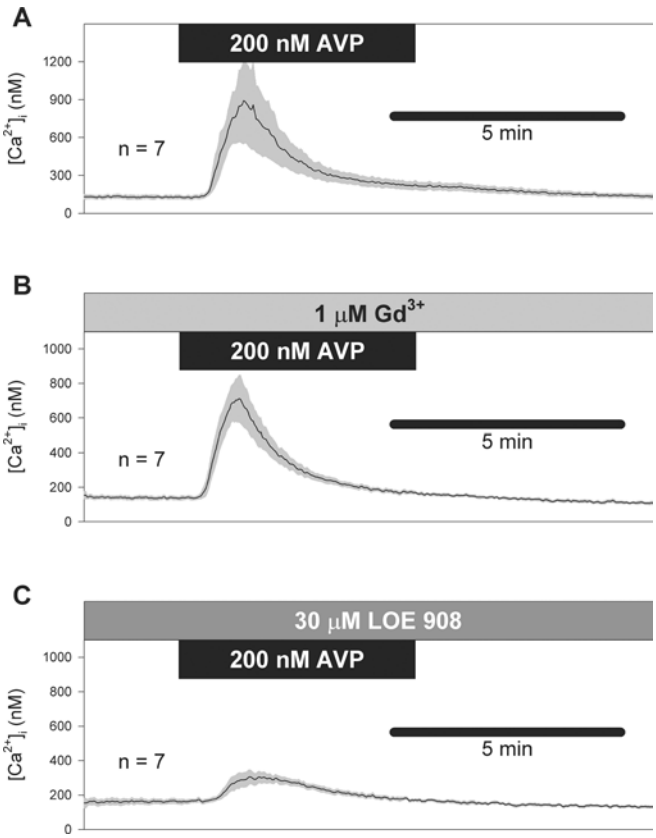

Figure 6 No rebound of Ca^{2+} entry after AVP removal

$[Ca^{2+}]_i$ responses to 200 nM AVP were measured by the method of Moneer and Taylor [3]. Mean responses (solid traces) ± S.E.M. (shaded error bars) are shown for AVP alone (**A**), AVP in the presence of Gd^{3+} (**B**) and AVP in the presence of LOE 908 (**C**). Note the absence of rebound transient on removal of AVP. As described by Moneer and Taylor [3], a V_{1a} vasopressin receptor antagonist ([β-mercapto-β,β-cyclopentamethylenepropionyl^1, O-Et-Tyr^2, Val^4, Arg^8]-vasopressin; 100 nM) was added at the time of AVP washout.

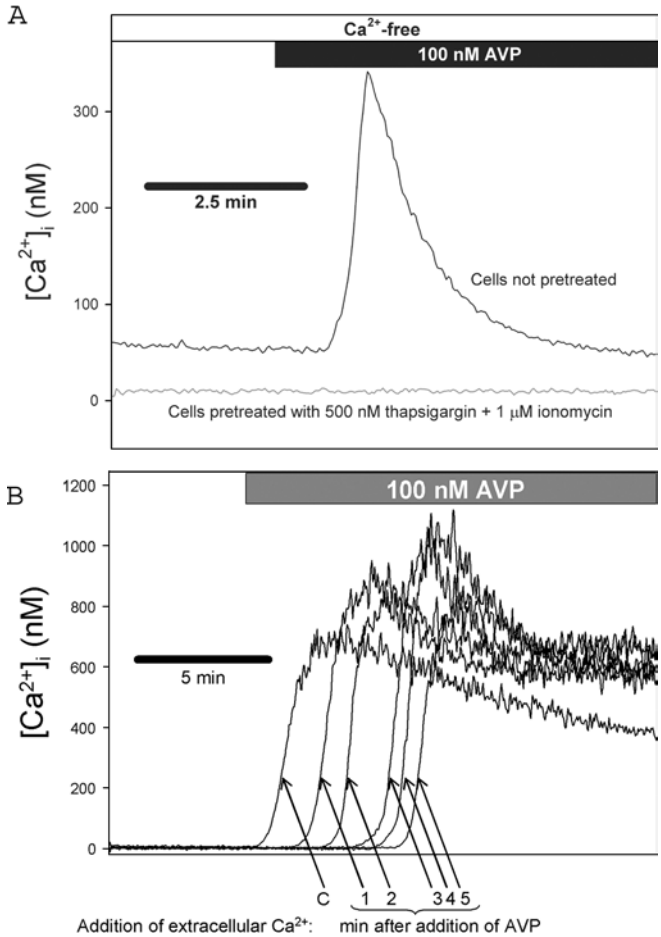

Figure 7 CCE is enhanced, not inhibited, by AVP

A7r5 cells were pretreated with 500 nM thapsigargin + 1 μM ionomycin in Ca^{2+}-free medium to deplete intracellular Ca^{2+} stores. (**A**) AVP-stimulated release of intracellular Ca^{2+} stores was estimated from fura 2 fluorescence (340:380 ratios) recorded from A7r5 cell populations during exposure to 100 nM AVP in Ca^{2+}-free medium in untreated controls (upper trace) or cells pretreated with 500 nM thapsigargin + 1 μM ionomycin (lower trace). These results demonstrate the effectiveness of the pretreatment for depletion of Ca^{2+} stores. (**B**) $[Ca^{2+}]_i$ was estimated from fura 2 fluorescence ratios (340:380) recorded during the reintroduction of extracellular Ca^{2+} (1.5 mM) without [arrow labelled 'C' or at various times (indicated below arrows) after the addition of 100 nM AVP]. Representative traces from individual coverslips are superimposed. Results are representative of three independent experiments.

entry, but neither enhances nor inhibits this cation-entry pathway once it has been maximally activated by passive store depletion. We also identify, for the first time in A7r5 cells, the electrophysiological equivalent of CCE, a store-operated cation current, which is activated by AVP or other treatments that result in the depletion of intracellular Ca^{2+} stores. This current (I_{SOC}) behaves in accordance with our fluorescence measurements of bivalent cation entry.

In several previous studies [13–16], I_{SOC} was not detected in A7r5 cells despite abundant evidence that CCE could be detected using fura 2 fluorescence. Iwamuro et al. [13], Iwasawa et al. [14], Jung et al. [15] and Nakajima et al. [16] failed to detect I_{SOC} at steady -40 to -60 mV holding potential in external solutions containing 0.2–1.8 mM Ca^{2+}. We were also unable to detect I_{SOC} under these conditions (results not shown). However, methods similar to those that we have used in the present study have been used by other investigators to detect store-operated currents in vascular smooth-muscle cells [17].

In A7r5 cells, I_{SOC} is a relatively Ca^{2+}-selective, inwardly rectifying, Gd^{3+}-sensitive cation current (Figures 1 and 2), which is distinct from at least two non-selective cation currents that may be detected in these cells (L. I. Brueggemann, L. L. Cribbs and K. L. Byron, unpublished work). Its identification as a store-operated current is based on: (i) its activation by passive store depletion independent of ligand–receptor interactions, e.g. by inhibition of sarco/endoplasmic reticulum Ca^{2+}-ATPase with thapsigargin or CPA or by dialysis with 10 mM BAPTA in a ruptured patch configuration; (ii) its pharmacological properties (Gd^{3+} sensitivity, LOE 908-insensitivity); and (iii) its ability to conduct Ca^{2+}. The pharmacological properties of I_{SOC} are consistent with fura 2 fluorescence measurements of CCE, which demonstrated that CCE was distinguished from NCCE by its sensitivity to low $[Gd^{3+}]$ [4] and its insensitivity to LOE 908 [3]. Its electrophysiological characteristics resemble those of I_{SOC} measured in vascular smooth-muscle cells by other investigators [17,18]. Furthermore, we found that I_{SOC} is significantly inhibited by treatment with an antisense construct to TRPC1 [19], a member of the transient receptor potential family of non-selective cation channels, which has been implicated by other investigators as a store-operated Ca^{2+} channel in vascular smooth muscles [20,21].

Activation of I_{SOC} by 100 nM AVP reproducibly reached a peak and then partially inactivated (Figures 1A and 2A). No inactivation of I_{SOC} was apparent after it was activated by passive store depletion with thapsigargin, CPA or BAPTA dialysis; nor

when AVP was applied after full activation of the current by thapsigargin (Figure 2B). A possible explanation for this observation is that partial refilling of the Ca^{2+} stores occurs during AVP treatment (this would tend to shut off the store-operated pathway and would not occur with the passive store depletion regimens or when AVP is added during thapsigargin treatment). Receptor desensitization might account for such an observation, but feedback inhibition on entry channels through a signalling pathway is an unlikely explanation because it would be expected to produce inactivation when AVP is added during thapsigargin treatment.

A reciprocal regulation model proposed by Moneer and Taylor [3] predicts that AVP should inhibit I_{SOC}. The activation of I_{SOC} by AVP and the absence of a rebound activation on AVP removal, combined with the observation that AVP did not inhibit thapsigargin-activated I_{SOC}, led us to re-examine the reciprocal regulation model, applying the fura 2 fluorescence methods used in the studies on which the model was based [3]. Our present findings are consistent with earlier studies of AVP-stimulated Ca^{2+} entry in A7r5 cells [1,4,5], but cannot be readily reconciled with the results of Moneer and Taylor [3] and Moneer et al. [6], which suggest that AVP inhibits store-operated Ca^{2+} or Mn^{2+} entry. We have not been able to reproduce some of the findings of Moneer et al. [3,6] despite our attempts to mimic as closely as possible the conditions described in their studies. For example, we did not observe any detectable rebound of $[Ca^{2+}]_i$ on AVP removal in the presence of LOE 908 (Figure 6C), whereas Figure 7(A) in [3] shows a huge rebound transient in which $[Ca^{2+}]_i$ reaches a peak at approx. 800 nM in amplitude. We observed an enhancement by AVP of the Ca^{2+} transient when extracellular Ca^{2+} was reintroduced to cells with depleted Ca^{2+} stores (Figure 7), whereas Figures 3(A) and 3(B) in [6] show that AVP completely abolishes this transient.

These contradictory findings suggest that something was different in the studies of Moneer et al. [3,6], but where that difference lies cannot be readily discerned from their description of the experimental design and methods. All of the methods for cell culture and fura 2 fluorescence appear to be essentially the same as those originally described by Byron and Taylor [7]. There were some subtle differences in the experimental design for measuring Mn^{2+} entry: in the experiments described by Moneer and Taylor [3], AVP was present for only 1 min and fluorescence quench rates were determined by regression analysis from only the final 20 s of that treatment. Other experiments by Moneer and Taylor [3] used much longer AVP treatments and indicated that the effects of AVP on CCE persisted for at least 5 min, so it is not clear why such a brief exposure was used for their Mn^{2+}-entry measurements. We have found that analysis of longer recordings (1–2 min) are necessary to obtain a linear regression with a correlation coefficient greater than 0.5 (in the present study, we excluded results with fits that did not meet this criterion) and that longer treatments are necessary to obtain stable quench rates (Figure 4). There is no evidence from the three earlier studies [1,4,5] or the present study that AVP inhibits CCE. In contrast, the results of Moneer et al. indicate that AVP does inhibit CCE. It is possible that the cells that were used by Moneer et al. represent a subpopulation of A7r5 cells with different properties, but the results from our analysis of single-cell responses do not identify any cell with the expected properties within our A7r5 cell population. If the reciprocal regulation phenotype has such a limited expression, the broad applicability of this model postulated by Taylor [22,23] may be questionable. The general stability of the A7r5 cell line does not appear to be in question because the cells used in the present study were derived from the same cells used throughout the 1990s by the Taylor laboratory [1,4,5,7] and the present results agree with the results of those earlier studies.

Reciprocal or co-ordinated regulation of multiple Ca^{2+}-entry pathways has been reported in several cell types and involving several agonist-stimulated signalling pathways (see discussion by Moneer and Taylor [3]). Most convincingly, activation of an NCCE pathway (ARC channels) by muscarinic agonists may be inhibited by sustained Ca^{2+} signals derived from store-operated Ca^{2+} entry at high agonist concentrations [24,25]. Our present findings do not rule out the possibility of such a co-ordinate regulation or the possibility that different Ca^{2+}-entry pathways may be activated by different concentrations of agonists, as suggested by early studies of AVP effects in A7r5 cells [1,2,4]. However, our findings do call into question the notion that CCE is inhibited by AVP in vascular smooth-muscle cells.

Regulation of Ca^{2+} entry in vascular smooth-muscle cells is of crucial importance to cardiovascular physiology since it regulates the contractile state of these cells and hence the diameter of blood vessels as a primary determinant of blood flow and blood pressure. Understanding how vasoconstrictor hormones regulate Ca^{2+} entry may provide a better understanding of cardiovascular diseases and improved therapeutic tools for the treatment of these diseases. Our findings bring to light a controversy in the literature of this field. Confirmation by independent laboratories may be required before additional weight is given to support or refute the reciprocal regulation model. In addition, new electrophysiological evidence such as that provided in the present study suggests a means to help resolve the controversy and understand the regulation of Ca^{2+} entry by vasopressin.

This work was supported by the John and Marian Falk Trust for Medical Research and the National Heart, Lung and Blood Institute (R01HL070670; to K. L. B.).

REFERENCES

1 Byron, K. L. and Taylor, C. W. (1995) Vasopressin stimulation of Ca^{2+} mobilization, two bivalent cation entry pathways and Ca^{2+} efflux in A7r5 rat smooth muscle cells. J. Physiol. (Cambridge, U.K.) **485**, 455–468

2 Byron, K. L. (1996) Vasopressin stimulates Ca^{2+} spiking activity in A7r5 vascular smooth muscle cells via activation of phospholipase A2. Circ. Res. **78**, 813–820

3 Moneer, Z. and Taylor, C. W. (2002) Reciprocal regulation of capacitative and non-capacitative Ca^{2+} entry in A7r5 vascular smooth muscle cells: only the latter operates during receptor activation. Biochem. J. **362**, 13–21

4 Broad, L. M., Cannon, T. R. and Taylor, W. (1999a) A non-capacitative pathway activated by arachidonic acid is the major Ca^{2+} entry mechanism in rat A7r5 smooth muscle cells stimulated with low concentrations of vasopressin. J. Physiol. (Cambridge, U.K.) **517**, 121–134

5 Broad, L. M., Cannon, T. R., Short, A. D. and Taylor, C. W. (1999b) Receptors linked to polyphosphoinositide hydrolysis stimulate Ca^{2+} extrusion by a phospholipase C-independent mechanism. Biochem. J. **342**, 199–206

6 Moneer, Z., Dyer, J. L. and Taylor, C. W. (2003) Nitric oxide co-ordinates the activities of the capacitative and non-capacitative Ca^{2+}-entry pathways regulated by vasopressin. Biochem. J. **370**, 439–448

7 Byron, K. L. and Taylor, C. W. (1993) Spontaneous Ca^{2+} spiking in a vascular smooth muscle cell line is independent of the release of intracellular Ca^{2+} stores. J. Biol. Chem. **268**, 6945–6952

8 Fan, J. and Byron, K. L. (2000) Ca^{2+} signalling in rat vascular smooth muscle cells: a role for protein kinase C at physiological vasoconstrictor concentrations of vasopressin. J. Physiol. (Cambridge, U.K.) **524**, 821–831

9 Wayman, C. P., McFadzean, I., Gibson, A. and Tucker, J. F. (1996) Two distinct membrane currents activated by cyclopiazonic acid-induced calcium store depletion in single smooth muscle cells of the mouse anococcygeus. Br. J. Pharmacol. **117**, 566–572

10 Hartzell, H. C. and Zhiqiang, Q. (2003) Chloride currents in acutely isolated Xenopus retinal pigment epithelial cells. J. Physiol. (Cambridge, U.K.) **549**, 453–469

11 Nilius, B. (2003) Calcium-impermeable monovalent cation channels: a TRP connection? Br. J. Pharmacol. **138**, 5–7

12 Kimes, B. W. and Brandt, B. L. (1976) Characterization of two putative smooth muscle cell lines from rat thoracic aorta. Exp. Cell Res. **98**, 349–366

13 Iwamuro, Y., Miwa, S., Zhang, X. F., Minowa, T., Enoki, T., Okamoto, Y., Hasegawa, H., Furutani, H., Okazawa, M., Ishikawa, M. et al. (1999) Activation of three types of voltage-independent Ca^{2+} channel in A7r5 cells by endothelin-1 as revealed by a novel Ca^{2+} channel blocker LOE 908. Br. J. Pharmacol. **126**, 1107–1114

14 Iwasawa, K., Nakajima, T., Hazama, H., Goto, A., Shin, W. S., Toyo-oka, T. and Omata, M. (1997) Effects of extracellular pH on receptor-mediated Ca^{2+} influx in A7r5 rat smooth muscle cells: involvement of two different types of channel. J. Physiol. (Cambridge, U.K.) **503**, 237–251

15 Jung, S., Strotmann, R., Schultz, G. and Plant, T. (2002) TRPC6 is a candidate channel involved in receptor-stimulated cation currents in A7r5 smooth muscle cells. Am. J. Physiol. Cell Physiol. **282**, C347–C359

16 Nakajima, T., Hazama, H., Hamada, E., Wu, S.-N., Igarashi, K., Yamashita, T., Seyama, Y., Omata, M. and Kurachi, Y. (1996) Endothelin-1 and vasopressin activate Ca^{2+}-permeable non-selective cation channels in aortic smooth muscle cells: mechanism of receptor-mediated Ca^{2+} influx. J. Mol. Cell. Cardiol. **28**, 707–722

17 Albert, A. P. and Large, W. A. (2002) A Ca^{2+}-permeable non-selective cation channel activated by depletion of internal Ca^{2+} stores in single rabbit portal vein myocytes. J. Physiol. (Cambridge, U.K.) **538**, 717–728

18 Curtis, T. M. and Scholfield, C. N. (2001) Nifedipine blocks Ca^{2+} store refilling through a pathway not involving L-type Ca^{2+} channels in rabbit arteriolar smooth muscle. J. Physiol. (Cambridge, U.K.) **532**, 609–623

19 Byron, K. L., Brueggemann, L. I. and Cribbs, L. L. (2004) TRPC1 antisense inhibits currents and Mn^{2+} entry activated by store-depletion in A7r5 vascular smooth muscle cells. FASEB. J. **18**, A305

20 Golovina, V. A., Platoshyn, O., Bailey, C. L., Wang, J., Limsuwan, A., Sweeney, M., Rubin, L. J. and Yuan, J. X. (2001) Upregulated TRP and enhanced capacitative Ca^{2+} entry in human pulmonary artery myocytes during proliferation. Am. J. Physiol. Heart Circ. Physiol. **280**, H746–H755

21 Sweeney, M., Yu, Y., Platoshyn, O., Zhang, S., McDaniel, S. S. and Yuan, J. X.-J. (2002) Inhibition of endogenous TRP1 decreases capacitative Ca^{2+} entry and attenuates pulmonary artery smooth muscle cell proliferation. Am. J. Physiol. Lung Cell. Mol. Physiol. **283**, L144–L155

22 Taylor, C. W. (2002) Controlling calcium entry. Cell (Cambridge, Mass.) **111**, 767–769

23 Taylor, C. W. (2002) Regulation of Ca^{2+} entry pathways by both limbs of the phosphoinositide pathway. Novartis Found. Sym. **246**, 91–101

24 Mignen, O., Thompson, J. L. and Shuttleworth, T. J. (2001) Reciprocal regulation of capacitative and arachidonate-regulated noncapacitative Ca^{2+} entry pathways. J. Biol. Chem. **276**, 35676–35683

25 Mignen, O., Thompson, J. L. and Shuttleworth, T. J. (2003) Calcineurin directs the reciprocal regulation of calcium entry pathways in nonexcitable cells. J. Biol. Chem. **278**, 40088–40096

Received 10 August 2004/13 December 2004; accepted 17 December 2004
Published as BJ Immediate Publication 17 December 2004, DOI 10.1042/BJ20041360